D. Instabilities of tokamaks

1) Ideal MHD modes [η=0, $t = O(10^{-6})$] : *Linear pert. theory, Energy principle*

a. Ideal kink modes

Driven by plasma currents j (∇j)

→ perturbation $\propto e^{i(m\Theta - n\phi)}$ ⇒ (m, n) mode

i) External modes

= Free surface modes (m=0 sausage, m=1 helical kink,
m=2, 3, ... surface kinks)

⇒ (m, n) modes fall on plasma surface r=a (vac. region),
i.e., mode rational surface $q(a) = m/n$

Fastest and most dangerous

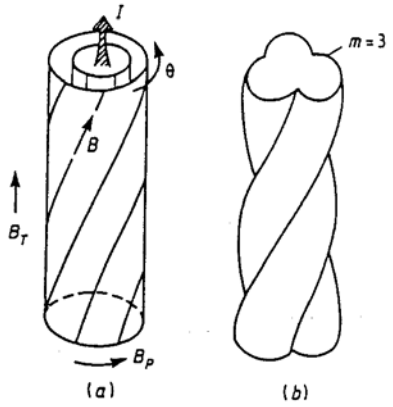

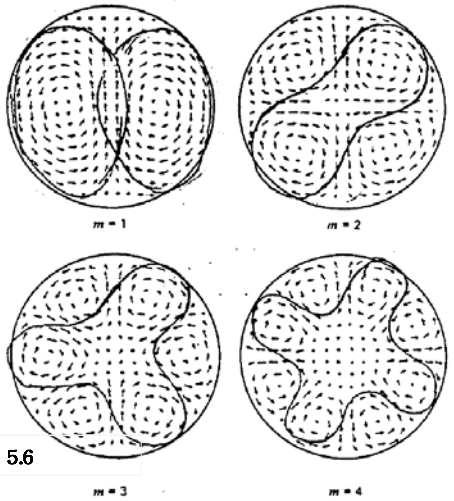

Gross[3] Fig. 5.6

Stablilizing effects and stability conditions :

① Conducting wall stabilization for low n modes

② Strong B_ϕ

③ $q(a) > m/n$ for (m, n) modes w/o conducting wall

Kruskal-Shafranov limit for m = n = 1 mode:

$$q(a) > 1 \quad \rightarrow \quad I_\phi \text{ limitation} \tag{36}$$

$$(e.g.) \quad I_\phi < \frac{2\pi B_\phi^o}{q(a)\mu_o}\left(\frac{a}{R_o}\right)^2 R \tag{37}$$

⇒ $R_o/a=3$, $R_o=11$ m, $B_\phi^o = 5\ T$ → $I_{max} \approx 12\ MA$

④ Centrally peaked $j_\phi(r)$ for m ≥ 2

$$\Rightarrow \quad \frac{q(a)}{q(0)} \geq \nu + 1 \approx 2\sim 3 \quad \text{for } j_\phi = j_o(1 - r^2/a^2)^\nu \tag{38}$$

For ν=0 (uniform), always unstable against any (m, n) mode

⑤ Magnetic shear (S $\propto \frac{i'}{i} = \frac{q'}{q}$)

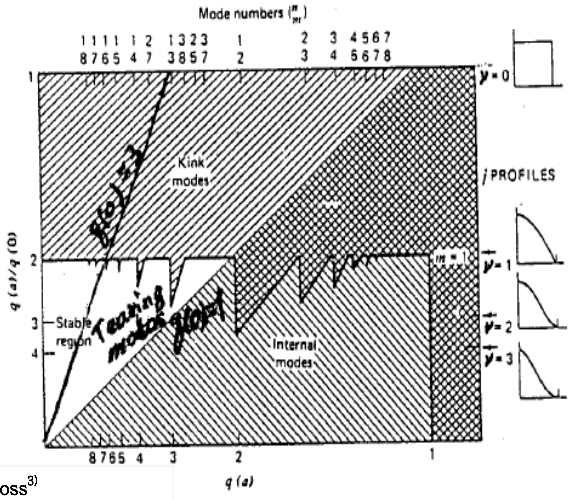

Gross[3)]

FIGURE 5.7. Stability diagram for ideal kink and internal modes of a large-aspect-ratio circular cross-section tokamak. The current distribution is $j_\phi(r) = j_\phi(0)(1 - r/a)^\nu$. Complete stability against kink modes may be obtained for any $q(a) > 1$ by sufficient peaking of the current profile (larger value of ν). The maximum stable current for this model is obtained with a parabolic current distribution with $q(0) = 1$ and $q(a) = 2$. (Data from J.A. Wesson [17].)

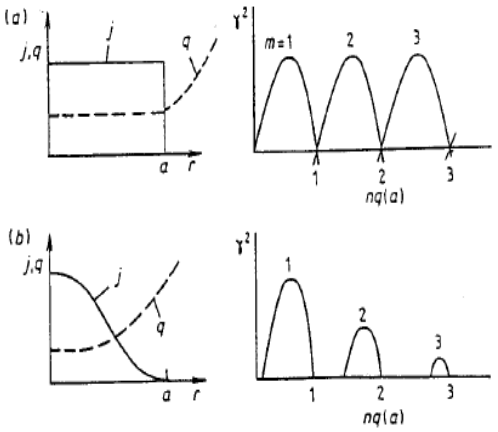

Figure 5.2 Growth rates of ideal MHD kink modes for different current density profiles: (*a*) homogeneous current density distribution; (*b*) natural current profile with decreased current density near the walls.

ii) Internal modes

Fixed boundary modes

∃ Singular surface inside plasma

Localized near rational surface r = r_s where $q(r_s) = m/n$

Stability condition for m=1, n=1 mode : **q(0) > 1** (39)

(m ≥ 2, ∀ n modes → stable)

b. Ideal interchange modes

Driven by ∇p

Internal modes : localized near mode rational surface r_s

where $q(r_s) = m/n$

No threat to confinement unless q(0) << 1

Stabilization :

① Min-B

② Magnetic shear

③ Mercier necessary condition

$$\left(\frac{q'}{q}\right)^2 + \frac{4}{r}\frac{P'}{B_\phi^2/2\mu_o}(1-q^2) > 0 \qquad (40)$$

⇒ q(r) > 1 for all r

shear stabilization ⇒ **q(0) > 1** (41)

(cf) Suydam criterion for cylindrical plasma

$$\left(\frac{q'}{q}\right)^2 + \frac{4}{r}\frac{P'}{B_\phi^2/2\mu_o} > 0 \qquad (42)$$

④ Elongated outward triangular cross section

c. Ideal ballooning modes

Driven by ∇p at bad-curvature surface region

Localized high-n interchange mode at outbound edge of circular high-β tokamak or at the tips of an elongated plasma

Most dangerous and limiting MHD instability

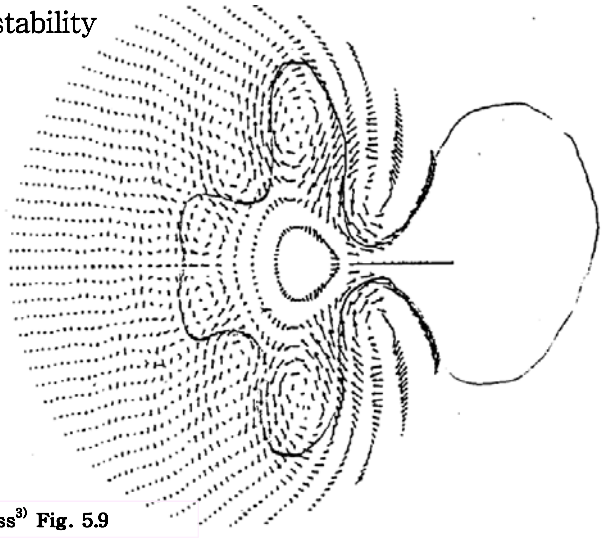

Gross[3] Fig. 5.9

5.9. Flow pattern for a tokamak ballooning mode with $n = 3$ at $(\beta^*) = 3\%$. Beta star

Stabilization :

- ∃ critical β above which ∃ ball. modes at any q values.

$$\beta < \beta_{max} \approx \frac{\varepsilon}{q^2} \qquad (43)$$

- Large R and $\nabla p(\propto 1/a)$ easily produce ball. modes → LAR
- Upper limit on n

$$\frac{nk(T_e+T_i)}{B^2/2\mu_o} < \frac{a}{q^2 R_o}$$

$$\Rightarrow \quad n < n_{max} \approx \frac{a}{6R_o}\frac{1}{k(T_e+T_i)}\frac{B^2}{2\mu_o} \qquad (44)$$

(e.g.) $R_0/a = 3$, $B = 9\ T$, $T_e = T_i = 10\ keV$

$\rightarrow$ $n_{max} \approx 5\times10^{20}\ m^{-3}$

- Upper limit on β

$\beta_{max} \uparrow$ as $\varepsilon \uparrow$, Elongation ↑ (noncircular), Conducting wall, Low n ↓ modes (W/ conducting wall)

Notes)

Limit on β due to ideal MHD instabilities :

$$\beta \equiv \frac{p}{B^2/2\mu_o} \approx \beta_p\left(\frac{B_\theta}{B_\phi}\right)^2 = \beta_p\left(\frac{a/R_o}{q(a)}\right)^2$$

$$= \left(\frac{a}{R_o}\beta_p\right)\left(\frac{a}{R_o}\right)\left(\frac{q(o)}{q(a)}\right)^2\left(\frac{1}{q(o)}\right)^2 \qquad (45)$$

① ② ③ ④

① ≤ 1 : ballooning modes limit

② ≤ ⅓ : space limit (geometry, shielding, maintenance, heating, etc)

③ ≤ 0.2 : surface kinks

④ ≤ 1 : internal modes

(cf) Energy principle ⇒

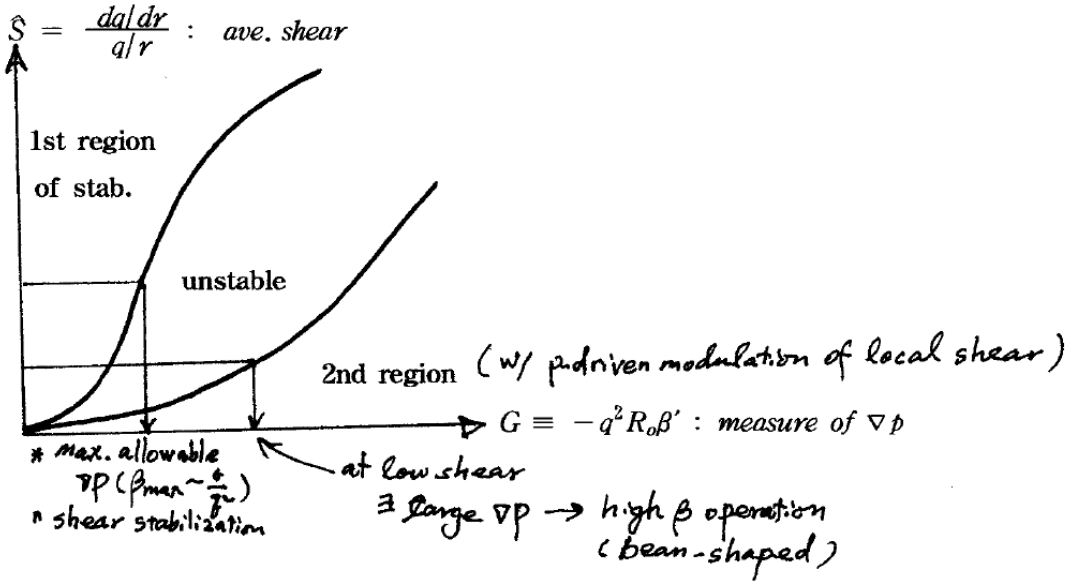

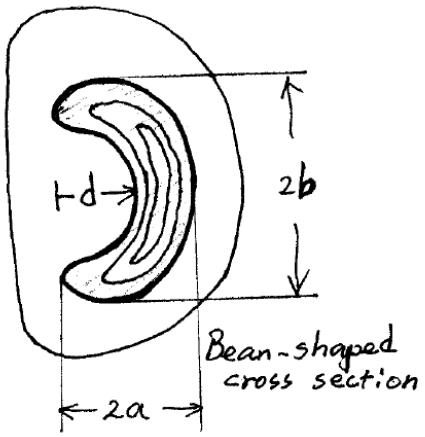

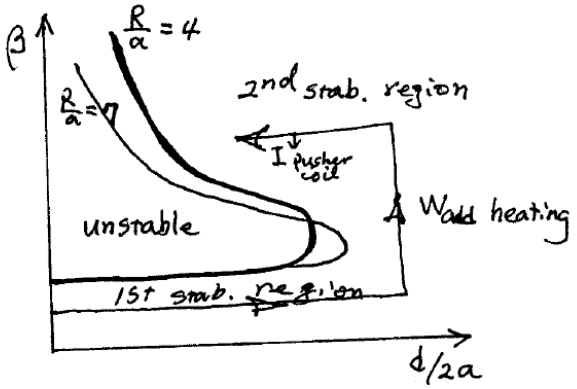

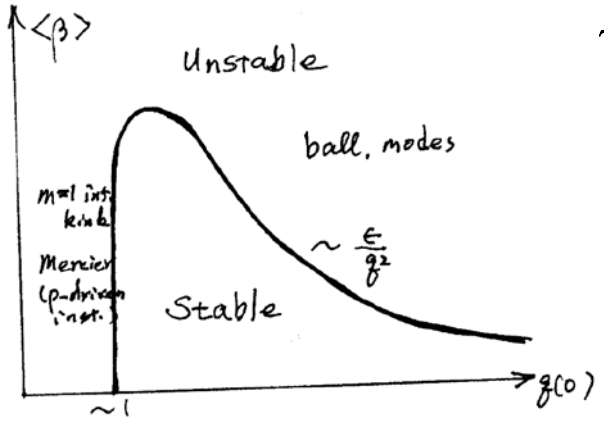

Troyon limit for { Mercier criterion
ballooning
m=1 internal kink
n=1 external ball. kink

$$\beta_{crit}(\%) = \beta_N \frac{I(MA)}{a(m)B(T)} \qquad (46)$$

where normalized $\beta_N \approx 2.8 \sim 5$

▶ *Troyon factor* C_T

2) Resistive MHD modes [$\eta \neq 0$, $t = O(10^{-4} \sim 10^{-2})$]

a. Tearing modes = Resistive internal kink modes ($m \geq 2$)

Driven by perturbed $\boldsymbol{B}$ induced by current layer (∇j) in plasma

Magnetic island formation (local pinch)

Mode rational surface r_s [$q(r_s) = m/n$] falls in plasma

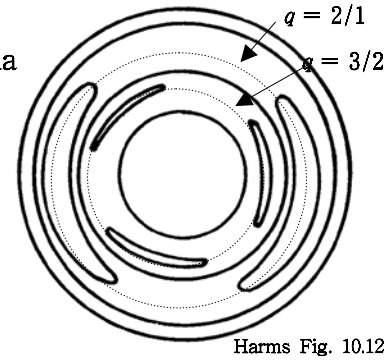

Harms Fig. 10.12

Saturation at some fraction of plasma width
(~ a few tenth of plasma radius a)

Growth rate $\gamma \propto \eta^{3/5}$

More tolerable & lower than ideal modes

Unstable region ↓ as sharfness of current profile ν ↑
m ↑
closeness of wall to plasma
[q(a)/q(0)] ↑ ; shear

Stability condition :

$$\mathbf{q(0) \geq 3} \qquad (47)$$

b. m=1 tearing mode

Always occurs late in the sequence of unstable modes whenever q(0) < 1
for m = n = 1

Independent of current profile

$\gamma \propto \eta^{1/3}$

c. Nonlinear tearing modes (Disruptive instability)

Nonlinear evolutions of resistive modes:

- Sawtooth oscillation (m = n = 1)
- Mirnov osc. : fish-bone (n = 1, m =1, 2, 3)
- Major dusruption (m = 2, n = 1 : trigger)

i) Internal disruption

(1,1) mode disruption

Observation of Sawtooth oscillation (soft X-ray, 2 ~20 keV)
Miranov oscillation (n=1, m=1,2,3 ...): Fish-bone mode

Enhanced energy transport in plasma center

Wessen[13] Fig.7.1.2

Sawtooth Oscillation

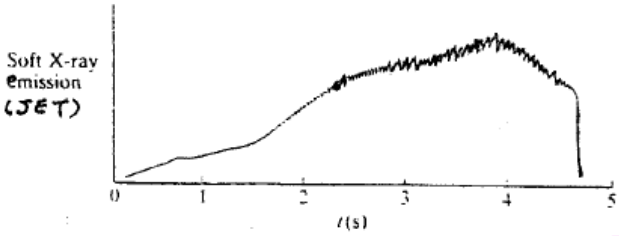

Wessen[13] Fig.7.6.4

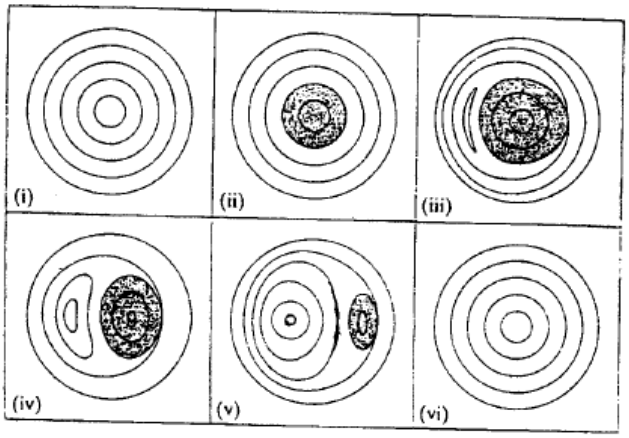

Possible development of the magnetic field structure during the rapid fall stage of the sawtooth instability. The $m = 1$ instability displaces the $q < 1$ region (shown shaded) and restores q_0 to a value >1.

Fish-bone oscillation

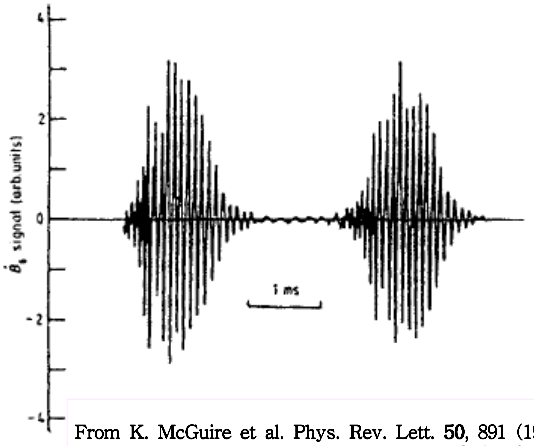

From K. McGuire et al. Phys. Rev. Lett. **50**, 891 (1983)

Oscillations of the poloidal-field time derivative as an indication of fish-bone instability

ii) Major disruption

Nonlinear evolution of m ≥ 2 tearing

(2, 1) mode triggering external disruption when q(0) < 1 & q(a) < 2.5

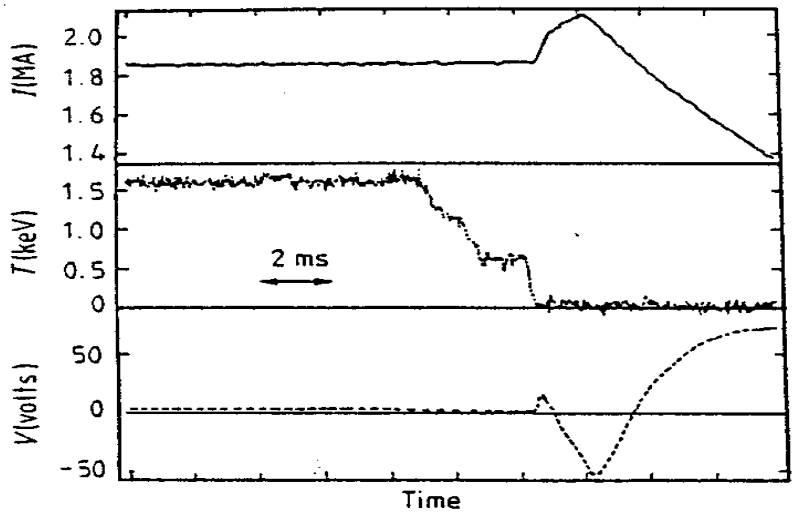

From J.A. Wessen et al. Nucl. Fusion **30**, 1011 (1990)

Termination of confinement:

Most dangerous and unpredictable

Large negative voltage spike in transformer

Damage to wall of PFCs

Rapid cooling of plasma

Hard X-ray burst

Plasma column shift

Control:

Keep I_ϕ and n within stable limits

Feedback control by helical coils

Additional heating to raise T_e

Close fitting conducting wall

d. Resistive interchange modes

Weaker stabilizing effect of shear

$\gamma \propto \eta^{1/3}$

Stable for m $\geq$ 4 for large tokamak

Stable even lower m($\leq$2) for reactor tokamak

3) *Microinstabilities*

Kinetic approach - limited MHD approach

Anomalous transports

a. Two-stream instability

Particle bunching $\rightarrow$ $\tilde{E}$ $\rightarrow$ bunching $\uparrow$ $\rightarrow$ unstable

b. Drift (or Universal) instability

Driven by ∇p (or ∇n) in B (with $k_\parallel \ll k_\perp$)

$\rightarrow$ Excitation of drift waves with $\omega / k_\perp = v_{De}$

Most unstable very short λ($k_\perp r_{Li} \approx 1$)

Anomalous transport $\rightarrow$ D_{Bohm}

Stabilization : Good curvature (min-B), Shear, Finite β

c. Trapped particle modes $\rightarrow$ cross-field diffusion $\uparrow$

Enhanced drift instability by trapped particle effects

Trapped electron mode (TEM)

Trapped ion mode (TIM)

Note)

No microinstability ($\omega \geq \Omega_i$)

due to velocity-space free energy (non-Maxwellian) in Tokamaks

E. Neoclassical transports

$$\Gamma = -D\nabla n \approx -\frac{(\Delta r)^2}{\tau}\nabla n \quad : \text{Fick's law}$$

$$q = -\kappa \nabla T \approx -\frac{(\Delta r)^2 n}{\tau_E}\nabla T \quad : \text{Fourier's law}$$

Thermal diffusivity :

$$\chi \equiv \frac{\kappa}{n} \approx \frac{(\Delta r)^2}{\tau_E} \approx D \quad \Rightarrow \quad \tau_E \approx \frac{a^2}{\chi}$$

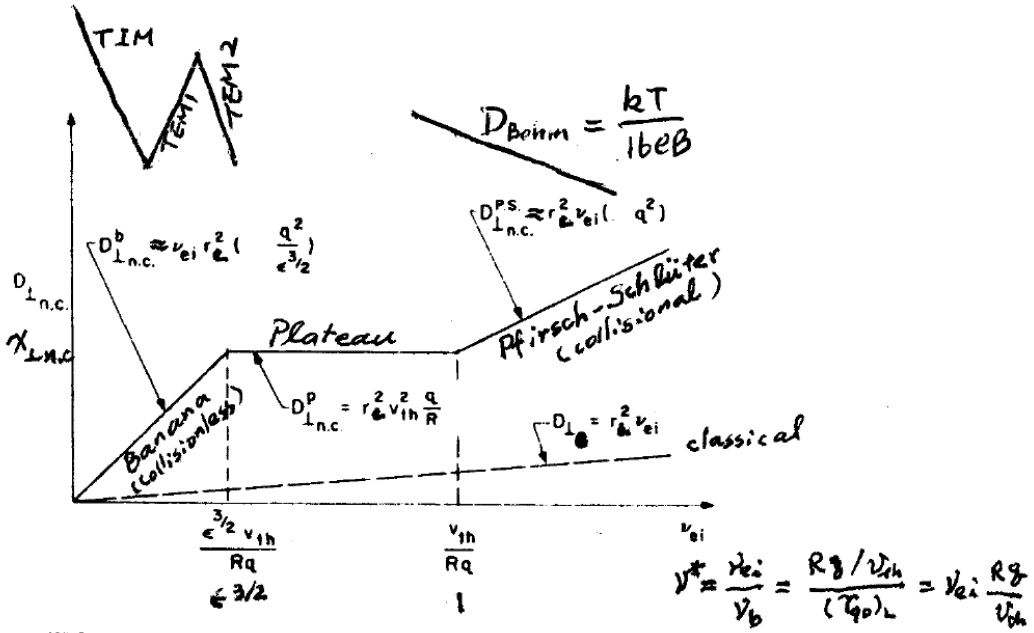

FIGURE 5.13. Neoclassical electron transport for tokamaks.

Bootstrap current - Toroidal current induced by radial NC diffusion in banana regime

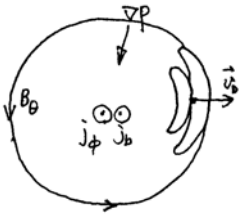

→ Direct consequence of banana toroidal drift combined with collisional diffusion

$$j_b \approx -\frac{\epsilon^{1/2}}{B_\theta}\frac{\partial p}{\partial r}$$

$$\frac{I_{BS}}{I} = 0.67\beta_p\sqrt{\epsilon}$$

→ Non-inductive current drive
Steady-state operation
Observed in TFTR, JT-60, JET (~89)

Comparison of NC results with experiments :

	τ	τ_E	χ
ions	×(wrong)	×	△(may agree)
electrons	×	×	×(O(1)~O(2))

F. Energy confinement time scaling ($\tau_E \equiv E_{th}/P_{heat}$)

Alcator scaling (75-82): OHT(Alcator A))

$$\tau_E = 5\times10^{-21}\,\overline{n_e}a^2$$

Neo-Alcator (82) : OHT(Alcator-C) $\tau_{NA} = 1.92\times10^{-21}\,\overline{n_i}aR^2$

Goldston (84) : AHT(TFTR) → L-mode (Low-confinement mode)

$$\tau_G = 3\times10^{-5} I_p R^{1.75} a^{-0.37} \kappa^{0.5} A_i^{0.5}/P_{aux}^{0.5}$$

ITER L-mode (89)

$$\tau_{ITER-89} = 0.048\, I^{0.85} R^{1.2} a^{0.3} n_{20}^{0.1} B^{0.2} (A_i \kappa_x / P(MW))^{0.5}$$

ITER H-mode (90) → H-mode (High-confinement mode)

$$\tau_{H-mode} \approx 2\sim3 \times \tau_{L-mode}$$

1984 ASDEX

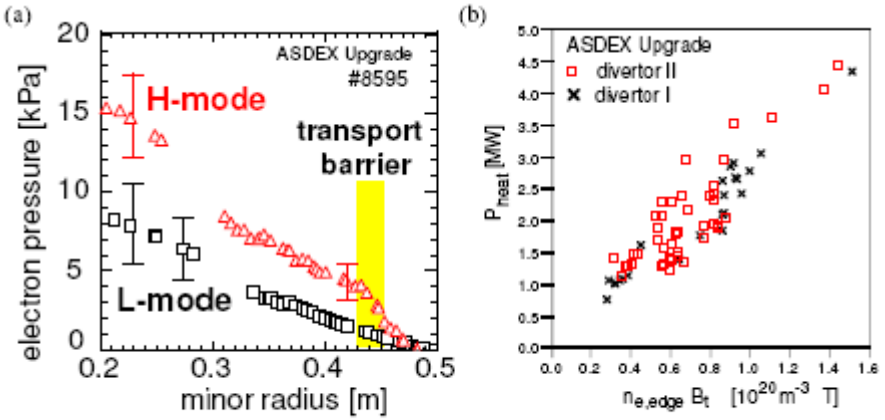

Figure 7.13: *(a) Comparison of electron pressure profiles in L-mode and H-mode, (b) Experimental power threshold for barrier formation* (W. Suttrop, MP-IPP Summer Univ. (2005))

International confinement database for a large set of tokamaks

$$\tau_{E,IPB98(y)} = 0.0365\, I(MA)^{0.97} B(T)^{0.08} P_{heat}(MW)^{-0.63} N_e (10^{19} m^{-3})^{0.41} M^{0.2} R(m)^{1.99} \epsilon^{0.23} \kappa^{0.67}$$

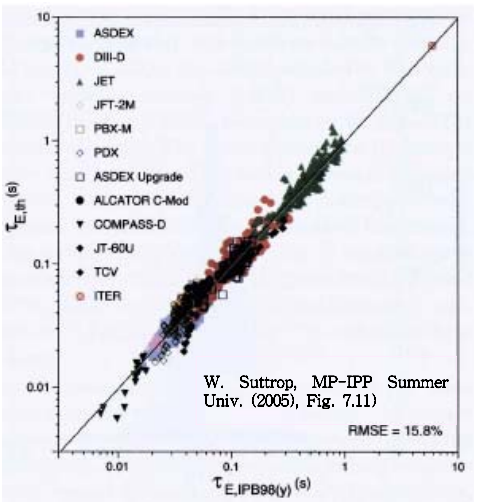

(cf) Different scaling laws caused by differences in geometry, impurity levels, ΔB, additional heatings, start-up & operation

(cf) Murakami empirical scaling law for density limitation for OHT (1976):

$$\overline{n_e}(m^{-3}) < (1-2)\times 10^{20}\frac{B_\phi(T)}{R(m)\,q_a}$$

Greewald density limit:

$$\overline{n}/10^{20} = \kappa\, J(MA/m^2) = I_{MA}/(\pi ab)$$

Hugill-Diagram

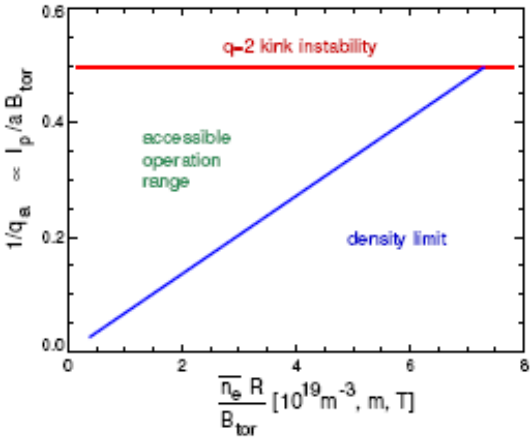

Figure 7.17: *Hugill-Diagram showing the basic tokamak operational range. An upper limit to the plasma current is given by the onset of $n = 1, m = 2$ kink instability for $q = 2$ at the plasma edge. A density limit exists at $\overline{n}_e \propto B_t/(Rq) \propto I_p/a^2$* (W. Suttrop, MP-IPP Summer Univ. (2005))

Advanced tokamak (AT) operation (Reversed shear by continuous bootstralp CD):

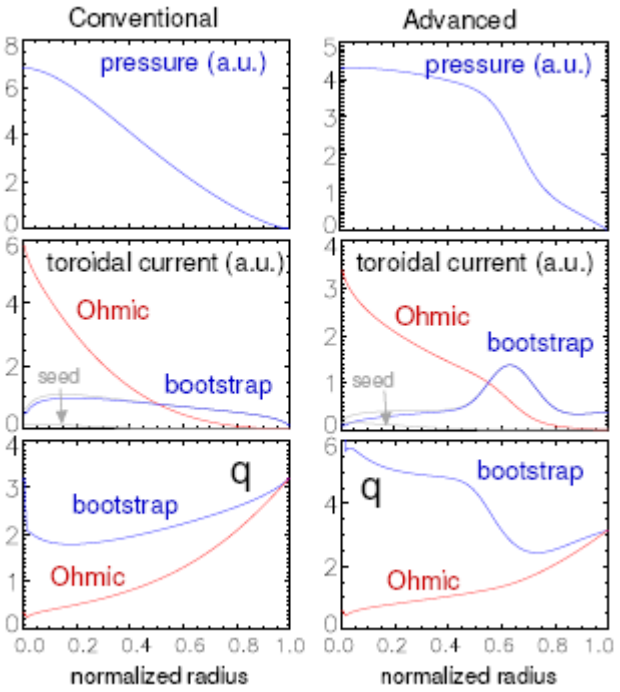

Figure 7.16: *Profiles of plasma pressure p, current density j and safety factor q comparing conventional and advanced scenarios. A conventional plasma has a monotonously rising q profile. Flat or reversed reversed q profile can lead to a transport barrier. In an ideal advanced scenario, the resulting steep pressure gradient creates a bootstrap current that maintains the q-profile non-inductively in steady state. Ohmic and bootstrap contributions to j and q are shown separately.* (W. Suttrop, MP-IPP Summer Univ. (2005))

Tokamaks in the World with $I_{plasma} \geq 1$ MA

Device	Institution/ Country	Geometry R (m) / a (m)	Elong-ation b/a	Plasma current I_p(MA)	Toroid-al field B_t (T)	Heating Power P_{add}(MW)	P /R (MW/m)	Max.press. ratio β_{max}(%)	Start of Operation
TFTR	PPPL/USA	2.5/0.85	1	2.5	5.2	32	13	1.7	1982 — 1998
JET	JET J.U./EU	2.96/1.2	1.8	7/ (6 div.)	3.5	>50	19.5	4.4	1983
DIII-D	GA/USA	1.67/0.67	2	3.5	2.2	20	12	5.1	1986
TORE SUPRA	EUR-CEA/ France	2.4/0.75	1	1.7	4.5	22	9.3	1.5	1988
T-15	Kurchatov/ Russ .Fed.	2.4/0.7	1	2	4	15	6.2	2.1	1988
FTU	EUR-ENEA/ Italy	0.93/0.31	1	≤1.6	8	≤9	8.5	1.9	1990
JT-60U	JAERI/ Japan	3.4/1.1	1.6	6	4.2	30	8.8	3.9	1991
ASDEX Upgrade	EUR-IPP/ Germany	1.65/0.5	1.6	≤1.6	3.9	≤28	≤16	2.5	1991
TCV	EUR-Suisse, CRPP/ Switzerland	0.88/0.24	3	<1.2	1.4	4.5	5.1	8.3	1992
ITER (project)	Europe, Japan, Russ. Fed., USA	8.1/2.8	1.6	21	5.7	100	39.5	3.2	(2008)

SNUT-79	SNU	0.65/0.15	1	0.12	3	OH			~85
KAIST-T (PRETEXT)	KAIST	0.53/0.15	1	0.08	10	OH			90
KT-1	KAERI	0.27/0.05	1	0.1	4	OH			86
KT-2	KAERI	1.4/0.25	1.8	0.5	3	ICRH/ECRH			(98)
KSTAR	KBSI	1.8/0.5	2.0	2.0	3.5	NBI/ICRH			2005